THE JOURNAL OF PHYSICAL CHEMISTRY Letters

Letter

pubs.acs.org/JPCL

Relation between Dephasing Time and Energy Gap Fluctuations in Biomolecular Systems

Maria Ilaria Mallus,[†] Mortaza Aghtar,[†] Suryanarayanan Chandrasekaran,[†] Gesa Lüdemann,[‡] Marcus Elstner,[‡] and Ulrich Kleinekathöfer*[,†]

[†]Department of Physics and Earth Sciences, Jacobs University Bremen, Campus Ring 1, 28759 Bremen, Germany

[‡]Institute of Physical Chemistry, Karlsruhe Institute of Technology, 76131 Karlsruhe, Germany

ABSTRACT: Excitation energy and charge transfer are fundamental processes in biological systems. Because of their quantum nature, the effect of dephasing on these processes is of interest especially when trying to understand their efficiency. Moreover, recent experiments have shown quantum coherences in such systems. As a first step toward a better understanding, we studied the relationship between dephasing time and energy gap fluctuations of the individual molecular subunits. A larger set of molecular simulations has been investigated to shed light on this dependence. This set includes bacterio-chlorophylls in Fenna–Matthews–Olson complexes, the PE545 aggregate, the LH2 complexes, DNA, photolyase, and cryptochromes. For the individual molecular subunits of these aggregates it has been confirmed quantitatively that an inverse proportionality exists between dephasing time and average gap energy fluctuation. However, for entire complexes including the respective intermolecular couplings, such a relation still needs to be verified.

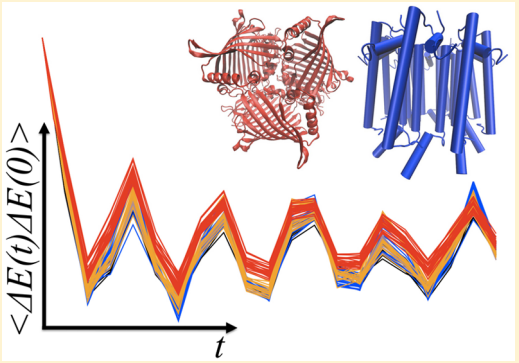

In biomolecular systems, the transfer of excitation energy and charges is ubiquitous. Quantum effects do play a major role in these processes; therefore, the amount of dephasing present in these system is also of quite some interest. It has been shown that coherence effects are important in charge[1,2] and excitation energy transfer.[3,4] Even in liquid water vibrational quantum coherence plays an interesting role.[5] Moreover, even in single pigments, dephasing is of key importance, as shown by two-dimensional electronic spectroscopy.[6,7] In all these systems the environment has two effects on the respective quantum (sub)system of interest: quantum coherences are washed out, and relaxation to the thermal equilibrium is enforced.

Coherences are usually associated with off-diagonal elements of density matrices and dephasing with the decrease of the coherences.[8] For electronic two-level systems with nuclear degrees of freedom, this dephasing is proportional to the so-called nuclear overlap/phase function.[9−11] Its absolute value is usually termed dephasing or decoherence function. This function is in turn used to define the pure dephasing time.[12,13] Up to an oscillatory phase factor, the dephasing function describes the time-dependent overlap of two initially identical nuclear wave packets evolving on two separate electronic states. Often these states are the ground and an excited state of the system of interest but, for example, can also be a neutral and ionized state. Initially, the overlap of the wave packets on the two surfaces equals unity, but due to the different forces acting on the nuclei on the two electronic surfaces, the overlap decreases with time. The probability of a revival is negligible because of the large number of atoms usually involved. In the Fermi Golden rule and the high-temperature approximation, the dephasing function has a purely Gaussian form.[12] In another approximation, a purely exponential decay for the dephasing function was obtained.[14] A comparison of these approximate functional dependencies to numerical results from molecular simulations is reported below.

The other important function in this study is the energy−energy autocorrelation function. By fitting its short-time behavior, for example, one can obtain the respective correlation time. Sometimes a proportionality between correlation and dephasing times is assumed,[15] while in a recent study the independence between the two time scales for some test systems was shown.[16] Moreover, these authors reported a surprising finding concerning their simulations of organic heterodimer molecules in different solvents. Plotting the pure dephasing times versus the corresponding average energy gap fluctuations resulted in a clear functional relationship between the two quantities. Furthermore, the dephasing time was found to be independent of the energy−energy autocorrelation time. It seems intuitive to some extent that a larger electron−nuclear correlation time leads to an enhanced dephasing time. That this assumption is not true is clear since the study by Akimov and Prezhdo.[16]

In the present study we are analyzing the relationship between dephasing time and the average energy gap fluctuation

Received: January 21, 2016
Accepted: March 7, 2016
Published: March 7, 2016

DOI: 10.1021/acs.jpclett.6b00134
J. Phys. Chem. Lett. 2016, 7, 1102−1108

for a much larger set of simulations. This data set is based on sequential combinations of molecular dynamics (MD) simulations and quantum chemistry calculations for the light-harvesting system II (LH2),[17] the Fenna-Matthews-Olson (FMO) trimer,[18,19] the PE545 system,[20] DNA,[21] photolyase,[22] and cryptochrome.[23] Because of the size of some of these systems, we do restrict ourselves to the analysis of the dephasing behavior for the individual subunits of the respective system, e.g., individual BChl *a* molecules in light-harvesting systems. As detailed below, the functional form found for these systems is different from the one found earlier by Akimov and Prezhdo.[16] Nevertheless, a clear functional dependence between the dephasing time and the electron−nuclear correlation time is found. This common behavior is traced back to common features of the energy−energy autocorrelation function.

Background on Dephasing Function and Time. For a better interpretation of our numerical results on molecular systems, we will analyze them within a generalized version of the stochastic line shape theory by Kubo[24] which was developed to describe homogeneous and inhomogeneous broadening in condensed phase spectroscopy. The time-dependent fluctuation of the energy gap is the key quantity in this expression. For the light-harvesting systems, we are concerned with the gap between ground and the (first) excited state, while for charge-transfer complexes the ionization energy, i.e., the energy difference between ionized and neutral state, is of interest. For simplicity we refrain here from adding site subscripts to all quantities like energy gap and correlation function because it should be clear that these always refer to a single chromophore. Therefore, for example, the energy gap will simply be denoted as $\Delta E = E - \langle E \rangle$. The average fluctuation along a trajectory can be characterized by

$$\langle \Delta E^2 \rangle^{1/2} = \sqrt{\langle \Delta E^2 \rangle - \langle \Delta E \rangle^2} \tag{1}$$

In Kubo's line shape theory the energy gap fluctuation is described by a Gaussian random process with mean value zero. Moreover, its autocorrelation function $C(t)$ is assumed to decay exponentially. Here we employ a generalized Kubo model with two different time scales.[25] In this model the unnormalized correlation function $C(t)$ consists of two parts with normalized prefactors α_1 and α_2, i.e., $\alpha_1+\alpha_2 = 1$, as well as correlation times $\tau_{c,1}$ and $\tau_{c,2}$

$$C(t) = \langle \Delta E^2 \rangle (\alpha_1 \exp(-t/\tau_{c,1}) + \alpha_2 \exp(-t/\tau_{c,2})) \tag{2}$$

The function $C(t)$ describes the correlation between the different electronic states which are functions of the time-dependent nuclear coordinates. Therefore, this function is also called the electron−nuclear correlation function. For the example of a light-harvesting 2 complex, we have shown earlier that the correlation function can reasonably be described by two exponential functions while the addition of damped oscillations makes an almost perfect fit possible.[17] Furthermore, from eq 2 one can deduce a general definition of the correlation time τ_c given by[26]

$$\tau_c = \frac{1}{\langle \Delta E^2 \rangle} \int_0^\infty C(t)\,\mathrm{d}t \tag{3}$$

For vanishing α_1 or α_2 in eq 2, this definition of the correlation time reproduces the respective correlation time. In Kubo's stochastic model, the line shape is defined as

$$I(\omega) = \frac{1}{\pi} \int_0^\infty \mathrm{d}t \cos(\omega t) \exp[-D(t)] \tag{4}$$

In this expression $D(t) \equiv \exp(-g(t))$ denotes the pure-dephasing function and can be expressed through the line shape function $g(t)$.[27] Within the cumulant approximation[28] the dephasing function is given by

$$D(t) \equiv \exp(-g(t)) = \exp\left[-\frac{1}{\hbar^2} \int_0^t \mathrm{d}\tau (t-\tau) \langle \Delta E(\tau)\, \Delta E(0) \rangle\right] \tag{5}$$

In addition to the simplified structure of the expression, the cumulant version of the dephasing function converges numerically much better than the original expression.[29] Moreover, this expression indicates that the dephasing is faster for larger correlation functions. As discussed above, the dephasing function describes the decoherence rate of a system due to the influence of the environmental fluctuations and is directly connected to the off-diagonal matrix elements of the respective density matrix.[9−11] The dephasing function is a key quantity for the present study, e.g., because it is used to define the dephasing time τ_D below. Using a sum of two exponentials as correlation function as given in eq 2, the line shape function reads

$$g(t) = \frac{\langle \Delta E^2 \rangle}{\hbar^2} \sum_{i=1}^{2} \alpha_i \tau_{c,i}{}^2 (\exp(-t/\tau_{c,i}) + t/\tau_{c,i} - 1) \tag{6}$$

Two limits for purely exponential correlation functions with correlation time τ_c are usually considered.[27] On the one hand, one can assume short correlation times $\tau_{c,1}$, i.e., $t \gg \tau_{c,1}$, corresponding to the homogeneus case. On the other hand, one obtains the inhomogeneus case in which the absorption line shape reflects a static distribution of frequencies in the limit of long correlation times $\tau_{c,2}$, i.e., $t \ll \tau_{c,2}$. Assuming that the fluctuations in the system under consideration include slow and fast fluctuations at the same time, the line shape function can be approximated by[25]

$$g(t) = \frac{\langle \Delta E^2 \rangle}{\hbar^2} (\alpha_1 \tau_{c,1} t + \alpha_2 t^2/2) \tag{7}$$

As defined above, the respective dephasing function is given by $D(t) = \exp(-g(t))$, while the dephasing time τ_D can now be defined as

$$\tau_D = \frac{2}{\sqrt{\pi}} \int_0^\infty D(t)\,\mathrm{d}t \tag{8}$$

This definition is similar, for example, to the definition of the correlation time as an integral over the normalized energy autocorrelation function.[11] The prefactor is chosen such that the standard definition of a dephasing time for a Gaussian dephasing function is reproduced[16] (see below). Calculating the dephasing time τ_D for the line shape function given in eq 7 leads to the following expression

$$\tau_D = \sqrt{\frac{2\hbar^2}{\langle \Delta E^2 \rangle \alpha_2}}\, \mathrm{e}^{-A\langle \Delta E^2 \rangle} \mathrm{erfc}\left(\sqrt{A\langle \Delta E^2 \rangle}\right) \tag{9}$$

In this equation, $\mathrm{erfc}(x)$ denotes the complementary error function and the constant A is given by

$$A = \frac{\tau_1^2}{2\hbar^2} \frac{\alpha_1^2}{\alpha_2} \tag{10}$$

DOI: 10.1021/acs.jpclett.6b00134
J. Phys. Chem. Lett. 2016, 7, 1102−1108

In the limit of vanishing α_1, i.e., a single-exponential correlation function with large correlation time, the Gaussian limit for the dephasing time is recovered[16]

$$\tau_{D,G} = \frac{B}{\sqrt{\langle \Delta E^2 \rangle}} \tag{11}$$

According to Kubo's theory,[24] the constant B has the value $B = \sqrt{2}\hbar$. However, Akimov and Prezhdo[16] argued that this value needs to be slightly enlarged when not employing the cumulant expansion of the dephasing function, leading to $B = \sqrt{12/5}\hbar$. Moreover, in the same study, an even larger value of $B = 1.82\hbar$ was obtained by fitting to their numerical data. Below we show that this latter value leads to an excellent agreement with our numerical data for charge-transfer systems as well.

Moreover, in the limit of vanishing α_2, i.e., a purely exponential correlation function with a short correlation time, the exponential limit for the dephasing time is obtained

$$\tau_{D,E} = \frac{2\hbar^2}{\sqrt{\pi}\tau_{c,1}\langle \Delta E^2 \rangle} \tag{12}$$

In this exponential case, the dephasing time is inversely proportional to the correlation time $\tau_{c,1}$ while in the former Gaussian case the dephasing time, eq 11, is completely independent of the respective correlation time $\tau_{c,2}$. This independence has been discussed earlier in ref 16 for a purely exponential correlation function. At this point we stress that the independence of $\tau_{D,G}$ from the long correlation time $\tau_{c,2}$ is also reflected in our generalized results, eq 9, because the value of A is independent of this quantity.

Results Based on Molecular Simulations. The dephasing times of heterodimers in simple fluids were at the focus of the investigation by Akimov and Prezhdo.[16] In the present study, simulations on a variety of systems are being analyzed, though we focus on the dephasing of the individual monomers. All results are based on a MD simulation and subsequent single-point quantum chemistry calculations either for the lowest excitation energy gap in the case of the exciton-transfer systems or for the ionization energy in the case of charge-transfer systems. For the MD simulations, either the CHARMM or AMBER force fields have been employed, while the quantum chemistry calculations were performed using the Zerner intermediate neglect of differential orbital (ZINDO), time-dependent density functional theory (TDDFT), and density functional-based tight binding (DFTB) approaches. The quantum chemistry predictions have all been performed as mixed quantum mechanical/molecular mechanical (QM/MM) calculations because the effect of the environmental fluctiations on the electronic structure determinations is of key importance as, for example, shown in ref 20. Table 1 lists the simulations together with the corresponding references in which all the details concerning the calculations are reported. Here we refrain from repeating all these simulation details because the purpose of the present study is to analyze these data in a way different from that done before.

The FMO and LH2 systems contain BChl *a* molecules as their functional subunits. Though the average energy gap fluctuations $\sqrt{\langle \Delta E^2 \rangle}$ of the individual pigments vary by about a factor of 2 (see below), the normalized correlation functions $\tilde{C}(t)$ show a large degree of similarity. As shown in Figure 1, these functions start with a sharp drop on a 5 fs time scale followed by a much slower decay combined with a fast oscillation with a period of around 20 fs. Certainly we cannot extract this time scale accurately from this plot because the time step in these simulations was 5 fs, i.e., our analysis of this data is restricted by this time step. The fast oscillations in the case of the BChls are connected to modes involving C═C and C═O double-bond vibrations.[31] The interesting part is to see that the normalized correlation functions do show very similar forms despite the different environments into which they are embedded. This finding strongly indicated that the normalized correlation function is to a large degree determined by the chemical structure of the investigated entity and not so much by its surroundings.

Table 1. List of the Eight Different Systems Investigated in This Study Together with Some Details and the Corresponding References[a]

number	system	sites	force field	energy gap	ref
1	FMO complex, *Chlorobaculum tepidum*	24	CHARMM	ZINDO	18
2	FMO complex, *Prosthecochloris aestuarii*	24	CHARMM	ZINDO	19
3	FMO complex, *P. aestuarii*	24	CHARMM	TDDFT	19
4	FMO Complex, *P. aestuarii*	24	AMBER	ZINDO	19
5	LH2 complex, *Rhodospirillum molischianum*	24	CHARMM	ZINDO	17
6	LH2 complex, *Rhodoblastus acidophila*	27	CHARMM	ZINDO	30
7	PE545 complex	8	AMBER	ZINDO	20
8	DNA	7	AMBER	DFTB	21
9	DNA Photolyase, *Escherichia coli*	6	AMBER	DFTB	22
10	Cryptochrome	3	AMBER	DFTB	23

[a] Moreover, the FMO complex from one bacterium has been calculated with two additional combinations of force field and quantum chemistry approach.

The PE545 complex contains bilin molecules instead of bacterio-chlorophylls, i.e., six phycoerythrobilins (PEBs) and two dihydrobiliverdins (DBVs).[20] As in the case of the BChl molecules, the normalized autocorrelation functions for the bilin molecules show a fast initial decay on a 5 fs time scale and fast oscillations with a period of around 20 fs. This finding is not surprising because the bilins do have quite some chemical similarity to BChl molecules. At the same time it is also clearly visible that the correlation functions of the two DBVs show larger oscillations around a slightly shifted curve compared to the PEBs. Four of the PEBs behave very similarly, while two of them show somewhat larger deviations. The enhanced resolution of the curves for the bilins compared to the BChl molecules in Figure 1 is due to the shorter time step in the underlying MD simulations of 2 fs compared to 5 fs.

In a next step we look at the dephasing functions as defined in eq 5. The integrals over the correlation functions in this expression need to be performed numerically. Here we note once more that because of the integration over the correlation function, its oscillatory features do not play a key role in the results below. Thus, the approximation of the correlation functions by a sum of two exponentially decaying functions as described above leads qualitatively to the same results. For some of the studied subunits the dephasing functions are shown in the inset of Figure 2. In the main part of the figure, we

DOI: 10.1021/acs.jpclett.6b00134
J. Phys. Chem. Lett. 2016, 7, 1102−1108

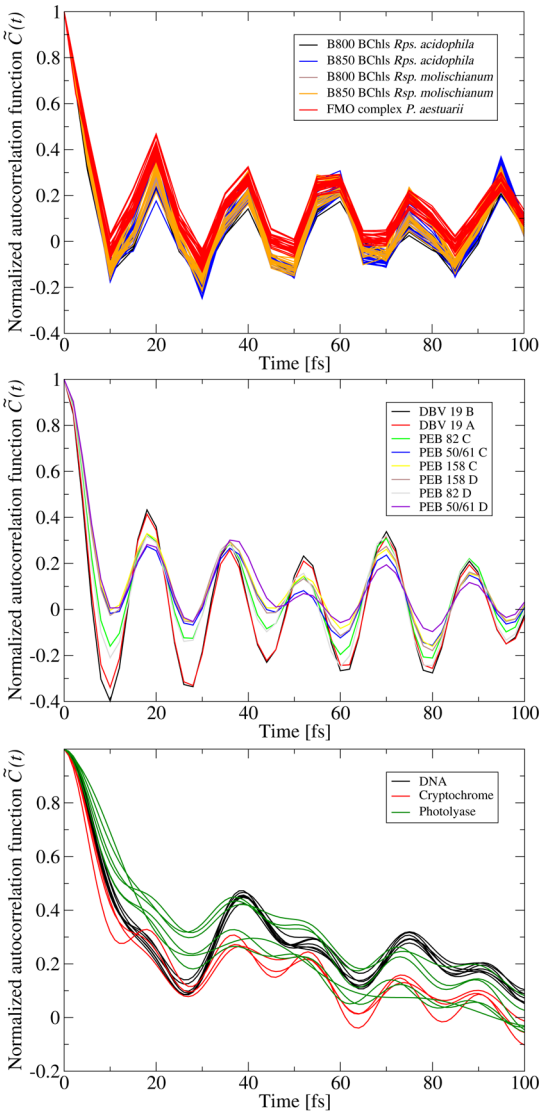

Figure 1. Normalized autocorrelation functions for BChls *a* (top panel), bilins (middle panel), and chargeable subunits (bottom panel) in different protein environments.

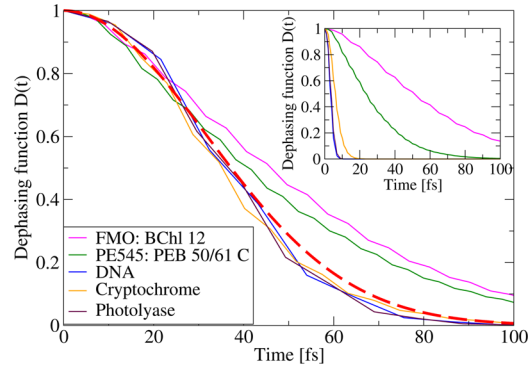

Figure 2. Different behavior of some example dephasing functions. In the inset, the unscaled dephasing functions are shown, while in the main panel the functions are scaled to have the same short-time behavior. The red dashed line represents a perfect Gaussian from.

have rescaled the dephasing functions of the different systems such that they overlap at short times. Due to the definition of the dephasing function, eq 5, all curves show a Gaussian behavior at very short times. For larger times, however, the curves for the examples from photosynthetic complexes, i.e., FMO and PE454, start to deviate from the Gaussian behavior while the curves corresponding to the charge-transfer systems DNA, cryptochrome, and photolyase exhibit quite Gaussian behavior. Please note that the dephasing functions of these charge-transfer systems decay much faster than those for the light-harvesting systems because of their larger fluctuations, i.e., stronger coupling to the environment. It is interesting to note, however, that for the excitonic heterodimers in simple fluids, Akimov and Prezhdo[16] found a purely Gaussian behavior.

Based on eq 8, the dephasing time can be determined by numerical integration from the corresponding dephasing function. Figure 3 depicts these dephasing times for individual

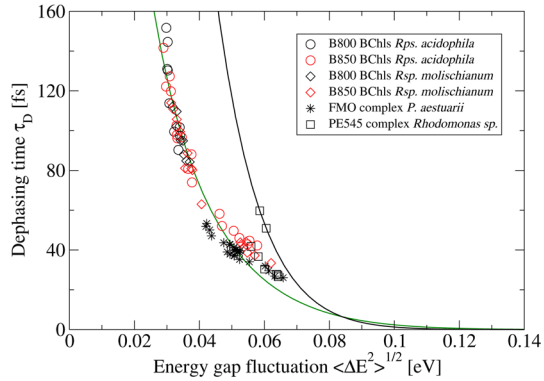

Figure 3. Dependence of the dephasing times on the electronic energy gap fluctuations for various light-harvesting systems. The green solid line is based on an almost exponential case with $A = 121$ and $\alpha_2 = 0.02$, while the black curve depicts a purely exponential case with $A = 225$ and $\alpha_2 = 0.0007$.

pigments of light-harvesting complexes as a function of the fluctuation of the energy gap function, $\langle \Delta E^2 \rangle^{1/2}$. All pigments of the respective complex are shown separately. It is very surprising to see that the results for almost all pigments lie on one curve. To better understand this numerical data we employed eq 9 with A and α_2 as fitting function for the bulk of the data, i.e., the data points for FMO and LH2 rings from *Rps. acidophila*. Thus, although the data from the LH2 rings of *Rsp. molischianum* were not included, their data points are very close to the fitted curve. The fit resulted in values of $A = 121$ and $\alpha_2 = 0.02$. In addition, included in this plot is a line for a purely exponential case with $\alpha_2 = 0.0007$ and an A value of $A = 225$. This curve is chosen to fit the data for the two points based on the exponential form which belongs to the DBV bilins from the PE545 complex. These two pigments indeed showed an exponential behavior of the dephasing function. The values of the parameters A and α_2 were obtained by fitting the numerical data points. Alternatively, one could fit the corresponding autocorrelation functions to a sum of two exponentials, eq 2, and thus obtain the parameters α_1, α_2, $\tau_{c,1}$, and $\tau_{c,2}$. With the help of eq 10, the value of A can be determined subsequently. The values of A obtained through the latter procedure differs from the value obtained through direct fitting roughly by a factor of 4. It is not surprising that one does not obtain exactly the same value because the correlation functions from the molecular simulations do contain the strong fast oscillations, which are neglected in the sum of two purely exponential functions. During the integration process to obtain the dephasing function, most of these oscillatory features are

DOI: 10.1021/acs.jpclett.6b00134
J. Phys. Chem. Lett. 2016, 7, 1102−1108

averaged out but not completely. Moreover, to obtain the line shape function in eq 7, we did further assume that the energy gap fluctuations contain very fast and slow components but none in the intermediate regime. Keeping these approximations in mind, it is rewarding to see that the values for A differ only by a factor of about four, indicating that the theory developed in the previous section does capture the main ingredients of the process.

In a next step we look at the dephasing in individual subunits of charge-transfer systems. One system consists of a double-stranded DNA heptamer with base sequence poly(dG)-poly(dC) in water.[21] Therefore, seven subunits of this system will be studied. The second system is the DNA photolyase.[22] Hole-transfer events in this aggregate are key steps in the photoactivation process, and six tryptophans in this compound have been studied. Moreover, three tryptophans in the structurally very similar cryptochrome complex were included in the analysis.[22] The normalized energy gap autocorrelation functions of these systems are shown in Figure 1 as well. The oscillations in this graph are not as pronounced as those of the previously discussed light-harvesting systems. Furthermore, the initial decay is slower. More importantly, however, is the fact that for the charge-transfer systems the energy gap fluctuations are much larger than those for the pigments of the light-harvesting systems. A change in the charge state of a molecular subunit couples much stronger to movements of charges in the environment than a rotation of a dipole moment in the case of a chromophore excitation. Therefore, the corresponding points in the diagram of dephasing times versus fluctuation of the energy gap function, $\langle \Delta E^2 \rangle^{1/2}$, lie in a rather different part of the parameter space. This part of the diagram is shown in Figure 4 where all subunits of the respective charge-transfer

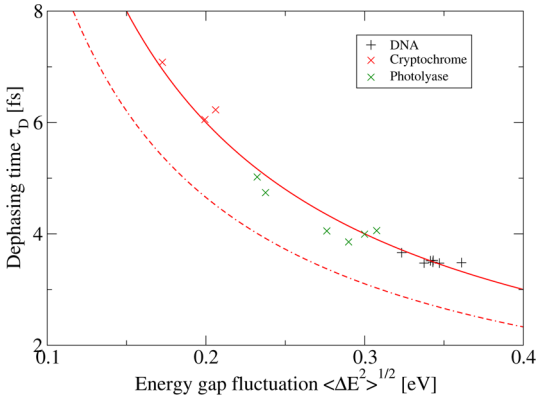

Figure 4. Dependence of the dephasing times on the electronic energy gap fluctuations for charge-transfer systems with purely Gaussian dephasing functions. The relation in eq 11 is used with the values $B = \sqrt{2}\hbar$ for the dashed line and $B = 1.82\hbar$ for the solid curve.

systems are depicted separately. Again, it is surprising that the results for subunits of the different charge-transfer systems lie on one curve. Shown in the graph is also the expression for the dephasing time in the Gaussian limit because the dephasing function in Figure 2 proved to be of Gaussian form. The equation for the dephasing time in this case, eq 11, contains the proportionality factor B. In Figure 4, two values for B are used. The factor resulting from the original Kubo theory $B = \sqrt{2}\hbar$ already leads to a reasonable agreement with the numerical data points, though an offset can be observed. Employing instead the value $B = 1.82\hbar$ as obtained by Akimov and Prezhdo[16] from their numerical data, the agreement between the analytic curve and the data points for realistic systems do agree very well, again supporting the overall theory employed in the present study.

One question is now how much the obtained results do depend on the level of theory which was used to obtain the numerical data points for the realistic systems in the present study. To this end, we employed two different MD force fields and two different quantum chemistry approaches. Recently we have performed a comparison for the FMO complex using the CHARMM or AMBER force fields, the ZINDO/S-CIS (Zerner intermediate neglect of differential orbital method with parameters for spectroscopic properties with single excitation configuration interaction) and TDDFT approaches for calculating the energy gaps and using different bacteria.[19] The results for dephasing time versus energy gap fluctuation for several of these combinations are shown in Figure 5. It is clearly

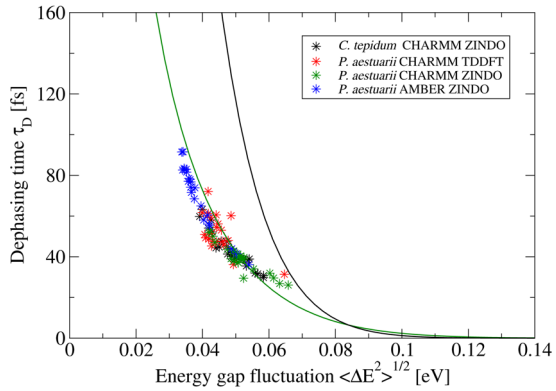

Figure 5. Independence of the relation between dephasing time and energy gap fluctuaction from methods used in the simulations.

visible that there is quite a spread in the results. These results, however, all lie on or close to the same curve which we already identified in Figure 4. These results show that the present finding does not strongly depend on the employed MD or quantum chemistry method but might, however, be influenced by our sequential scheme of performing the energy gap calculations on a predetermined MD trajectory. The effects of polarization in the QM/MM approach[32,33] or of ab initio MD[34] need to be investigated as well. Furthermore, this result supports the fact that the normalized correlation functions are basically influenced by the molecular structure of the studied subunit and not so much by its surroundings. This "molecular fingerprint" in turn leads to the observed relation between dephasing time and average gap fluctuations.

In this study we have shown that for BChl *a* molecules in different protein environments the respective normalized autocorrelation functions show a large degree of similarity and can be seen as a kind of "molecular fingerprint". These functions have a fast initial decay on a 5 fs time scale as well as oscillations on the 20 fs time scale. Assuming that these correlation functions can be approximated by a sum of two exponential functions, one with a fast and one with a long decay time, we were able to derive an expression for the dephasing time as a function of the average energy gap fluctuation. The data from the molecular simulations can be fitted accurately with this functional form. Moreover, the calculation of the respective parameters in this function directly from a fit of the autocorrelation functions to sums of two exponential functions

DOI: 10.1021/acs.jpclett.6b00134
J. Phys. Chem. Lett. 2016, 7, 1102−1108

yields similar but not identical values, which is not surprising taking into account the underlying assumptions. Nevertheless, with this generalized Kubo formalism we can understand that the dephasing times for BChl *a* molecules in various protein systems show a unique functional dependence as a function of energy gap fluctuation. The PEB bilins from the PE545 complex show autocorrelation functions very similar to those of the BChl *a* molecules and actually follow the same behavior. For the DBV bilins from the same complex, we can see distinctly larger oscillations in the correlation function leading to a different functional behavior for the dephasing time. The average energy gap fluctuations are much larger for the studied charge-transfer systems. On the basis of the generalized Kubo model, we can understand that in this case the dephasing time becomes much more independent of the details of the normalized correlation function.

It is interesting to note that the analytic formula for the dephasing time obtained from the generalized Kubo theory does not depend on the long time scale $\tau_{c,2}$ of the autocorrelation function. This finding is consistent with earlier results for simpler systems showing purely Gaussian dephasing functions.[16] This long time scale $\tau_{c,2}$, however, severely influences the low-frequency part of the spectral density, which is basically a half-sided Fourier transform of the autocorrelation function.[20,35−37] This low-frequency part of the spectral density is actually very important for the dephasing and exciton-transfer dynamics in the full complex in which small energies between excitonic states of the full complex play a major role.[19,38,39] Therefore, we need to emphasize that the dephasing times determined in the present study are those for the individual chromophores and not the complete complexes. Further investigations are needed to unravel the connection of the present findings and the observed long-lived quantum coherences in detail. The present study, however, yields important insight into the behavior of individual pigments and their similarities in different protein environments. It remains to be seen how much the present findings can be applied to other molecular and nanoscopic objects, such as quantum dots,[29] clusters,[40] and nanocrystals.[41]

AUTHOR INFORMATION

Corresponding Author

*E-mail: u.kleinekathoefer@jacobs-university.de.

Notes

The authors declare no competing financial interest.

ACKNOWLEDGMENTS

This work has been supported by Grant KL 1299/12-1 of the Deutsche Forschungsgemeinschaft (DFG).

REFERENCES

(1) Narth, C.; Gillet, N.; Cailliez, F.; Levy, B.; de la Lande, A. Electron Transfer, Decoherence, and Protein Dynamics: Insights from Atomistic Simulations. *Acc. Chem. Res.* **2015**, *48*, 1090−1097.

(2) Beratan, D. N.; Liu, C.; Migliore, A.; Polizzi, N. F.; Skourtis, S. S.; Zhang, P.; Zhang, Y. Charge Transfer in Dynamical Biosystems, or The Treachery of (Static) Images. *Acc. Chem. Res.* **2015**, *48*, 474−481.

(3) Fassioli, F.; Dinshaw, R.; Arpin, P. C.; Scholes, G. D. Photosynthetic Light Harvesting: Excitons and Coherence. *J. R. Soc., Interface* **2014**, *11*, 20130901.

(4) Dahlberg, P. D.; Norris, G. J.; Wang, C.; Viswanathan, S.; Singh, V. P.; Engel, G. S. Coherences Observed in Vivo in Photosynthetic Bacteria Using Two-dimensional Electronic Spectroscopy. *J. Chem. Phys.* **2015**, *143*, 101101.

(5) Joutsuka, T.; Thompson, W. H.; Laage, D. Vibrational Quantum Decoherence in Liquid Water. *J. Phys. Chem. Lett.* **2016**, *7*, 616−621.

(6) Wells, K. L.; Zhang, Z.; Rouxel, J. R.; Tan, H.-S. Measuring the Spectral Diffusion of Chlorophyll a Using Two-Dimensional Electronic Spectroscopy. *J. Phys. Chem. B* **2013**, *117*, 2294−2299.

(7) Moca, R.; Meech, S. R.; Heisler, I. A. Two-Dimensional Electronic Spectroscopy of Chlorophyll a: Solvent Dependent Spectral Evolution. *J. Phys. Chem. B* **2015**, *119*, 8623−8630.

(8) May, V.; Kühn, O. *Charge and Energy Transfer in Molecular Systems*, 3rd ed.; Wiley-VCH: Berlin, 2011.

(9) Lockwood, D. M.; Hwang, H.; Rossky, P. J. Electronic Decoherence in Condensed Phases. *Chem. Phys.* **2001**, *268*, 285−293.

(10) Hwang, H.; Rossky, P. J. An Analysis of Electronic Dephasing in the Spin-boson Model. *J. Chem. Phys.* **2004**, *120*, 11380−11385.

(11) Hwang, H.; Rossky, P. J. Electronic Decoherence Induced by Intramolecular Vibrational Motions in a Betaine Dye Molecule. *J. Phys. Chem. B* **2004**, *108*, 6723−6732.

(12) Prezhdo, O. V.; Rossky, P. J. Evaluation of Quantum Transition Rates from Quantum-classical Molecular Dynamics Simulations. *J. Chem. Phys.* **1997**, *107*, 5863−5878.

(13) de la Lande, A.; Řezáč, J.; Lévy, B.; Sanders, B. C.; Salahub, D. R. Transmission Coefficients for Chemical Reactions with Multiple States: Role of Quantum Decoherence. *J. Am. Chem. Soc.* **2011**, *133*, 3883−3894.

(14) Jasper, A. W.; Truhlar, D. G. Electronic decoherence time for non-Born-Oppenheimer trajectories. *J. Chem. Phys.* **2005**, *123*, 064103.

(15) Souaille, M.; Marchi, M. Nuclear Dynamics and Electronic Transition in a Photosynthetic Reaction Center. *J. Am. Chem. Soc.* **1997**, *119*, 3948−3958.

(16) Akimov, A. V.; Prezhdo, O. V. Persistent Electronic Coherence Despite Rapid Loss of Electron-Nuclear Correlation. *J. Phys. Chem. Lett.* **2013**, *4*, 3857−3864.

(17) Olbrich, C.; Kleinekathöfer, U. Time-dependent Atomistic View on the Electronic Relaxation in Light-harvesting System II. *J. Phys. Chem. B* **2010**, *114*, 12427−12437.

(18) Aghtar, M.; Strümpfer, J.; Olbrich, C.; Schulten, K.; Kleinekathöfer, U. The FMO Complex in a Glycerol-Water Mixture. *J. Phys. Chem. B* **2013**, *117*, 7157−7163.

(19) Chandrasekaran, S.; Aghtar, M.; Valleau, S.; Aspuru-Guzik, A.; Kleinekathöfer, U. Influence of Force Fields and Quantum Chemistry Approach on Spectral Densities of BChl a in Solution and in FMO Proteins. *J. Phys. Chem. B* **2015**, *119*, 9995−10004.

(20) Aghtar, M.; Strümpfer, J.; Olbrich, C.; Schulten, K.; Kleinekathöfer, U. Different Types of Vibrations Interacting with Electronic Excitations in Phycoerythrin 545 and Fenna-Matthews-Olson Antenna Systems. *J. Phys. Chem. Lett.* **2014**, *5*, 3131−3137.

(21) Kubař, T.; Kleinekathöfer, U.; Elstner, M. Solvent Fluctuations Drive the Hole Transfer in DNA: a Mixed Quantum-Classical Study. *J. Phys. Chem. B* **2009**, *113*, 13107−13117.

(22) Lüdemann, G.; Woiczikowski, P. B.; Kubař, T.; Elstner, M.; Steinbrecher, T. B. Charge Transfer in *E. coli* DNA Photolyase: Understanding Polarization and Stabilization Effects via QM/MM Simulations. *J. Phys. Chem. B* **2013**, *117*, 10769−10778.

(23) Lüdemann, G.; Solov'yov, I. A.; Kubař, T.; Elstner, M. Solvent Driving Force Ensures Fast Formation of a Persistent and Well-Separated Radical Pair in Plant Cryptochrome. *J. Am. Chem. Soc.* **2015**, *137*, 1147−1156.

(24) Kubo, R. Stochastic Theory of Line Shape. In *Fluctuation, Relaxation and Resonance in Magnetic Systems*; Oliver and Boyd: Edinburgh, 1962; pp 23−68.

(25) Schmidt, J.; Sundlass, N.; Skinner, J. Line Shapes and Photon Echoes within a Generalized Kubo Model. *Chem. Phys. Lett.* **2003**, *378*, 559−566.

(26) Schatz, G. C.; Ratner, M. *Quantum Mechanics in Chemistry*; Prentice Hall: Englewood Cliffs, NJ, 1993.

(27) Hamm, P.; Zanni, M. *Concepts and Methods of 2D Infrared Spectroscopy*; Cambridge University Press: Cambridge, 2011.

DOI: 10.1021/acs.jpclett.6b00134
J. Phys. Chem. Lett. 2016, 7, 1102−1108

(28) Mukamel, S. *Principles of Nonlinear Optical Spectroscopy*; Oxford University Press: New York, 1995.
(29) Liu, J.; Kilina, S. V.; Tretiak, S.; Prezhdo, O. V. Ligands Slow Down Pure-Dephasing in Semiconductor Quantum Dots. *ACS Nano* **2015**, *9*, 9106−9116.
(30) Mallus, I.; Aghtar, M.; Kleinekathöfer, U. To be submitted for publication, 2016.
(31) Ceccarelli, M.; Procacci, P.; Marchi, M. An Ab Initio Force Field for the Cofactors of Bacterial Photosynthesis. *J. Comput. Chem.* **2003**, *24*, 129−132.
(32) Curutchet, C.; Kongsted, J.; Munoz Losa, A.; Hossein Nejad, H.; Scholes, G. D.; Mennucci, B. Photosynthetic Light-harvesting Is Tuned by the Heterogeneous Polarizable Environment of the Protein. *J. Am. Chem. Soc.* **2011**, *133*, 3078−3084.
(33) Jurinovich, S.; Curutchet, C.; Mennucci, B. The Fenna-Matthews-Olson Protein Revisited: A Fully Polarizable (TD)DFT/MM Description. *ChemPhysChem* **2014**, *15*, 3194−3204.
(34) Rosnik, A. M.; Curutchet, C. Theoretical Characterization of the Spectral Density of the Water-Soluble Chlorophyll-Binding Protein from Combined Quantum Mechanics/Molecular Mechanics Molecular Dynamics Simulations. *J. Chem. Theory Comput.* **2015**, *11*, 5826−5837. PMID: 26610205.
(35) Damjanović, A.; Kosztin, I.; Kleinekathöfer, U.; Schulten, K. Excitons in a Photosynthetic Light-harvesting System: A Combined Molecular Dynamics, Quantum Chemistry and Polaron Model Study. *Phys. Rev. E: Stat. Phys., Plasmas, Fluids, Relat. Interdiscip. Top.* **2002**, *65*, 031919.
(36) Olbrich, C.; Strümpfer, J.; Schulten, K.; Kleinekathöfer, U. Theory and Simulation of the Environmental Effects on FMO Electronic Transitions. *J. Phys. Chem. Lett.* **2011**, *2*, 1771−1776.
(37) Jurinovich, S.; Viani, L.; Curutchet, C.; Mennucci, B. Limits and Potentials of Quantum Chemical Methods in Modelling Photosynthetic Antennae. *Phys. Chem. Chem. Phys.* **2015**, *17*, 30783−30792.
(38) Olbrich, C.; Jansen, T. L. C.; Liebers, J.; Aghtar, M.; Strümpfer, J.; Schulten, K.; Knoester, J.; Kleinekathöfer, U. From Atomistic Modeling to Excitation Dynamics and Two-dimensional Spectra of the FMO Light-harvesting Complex. *J. Phys. Chem. B* **2011**, *115*, 8609−8621.
(39) Aghtar, M.; Kleinekathöfer, U. Environmental Coupling and Population Dynamics in the PE545 Light-harvesting Complex. *J. Lumin.* **2016**, *169*, 406−409.
(40) Liu, J.; Neukirch, A. J.; Prezhdo, O. V. Phonon-induced Pure-dephasing of Luminescence, Multiple Exciton Generation, and Fission in Silicon Clusters. *J. Chem. Phys.* **2013**, *139*, 164303.
(41) Dong, S.; Trivedi, D.; Chakrabortty, S.; Kobayashi, T.; Chan, Y.; Prezhdo, O. V.; Loh, Z.-H. Observation of an Excitonic Quantum Coherence in CdSe Nanocrystals. *Nano Lett.* **2015**, *15*, 6875−6882.

DOI: 10.1021/acs.jpclett.6b00134
J. Phys. Chem. Lett. 2016, 7, 1102−1108